JSHC
Japan Society of Histochemistry and Cytochemistry
Established 1959

Acta Histochem. Cytochem. 59 (1): 1–11, 2026
doi: 10.1267/ahc.25-00065

Review

Spatial Transcriptomics Meets Histochemistry: Insights from Glioblastoma as a Model System

Syuri Tomioka[1], Riko Kitazawa[1,2], Ryuma Haraguchi[1], Yuki Takaoka[1], Akihiro Inoue[3] and Sohei Kitazawa[1]

[1]Department of Molecular Pathology, Ehime University Graduate School of Medicine, Toon, Ehime, Japan, [2]Division of Diagnostic Pathology, Ehime University Hospital, Toon, Ehime, Japan and [3]Department of Neurosurgery, Ehime University Graduate School of Medicine, Toon, Ehime, Japan

Received December 23, 2025; accepted January 1, 2026; published online February 17, 2026

High-resolution spatial transcriptomics has emerged as a powerful approach for linking genome-wide gene expression with preserved tissue architecture, enabling new insights into cellular heterogeneity and microenvironmental organization in complex tissues. In neuropathology, where morphological context is central to disease interpretation, these technologies are particularly appealing. Using glioblastoma multiforme (GBM) as a representative and highly heterogeneous model, this review critically evaluates the strengths and limitations of high-resolution spatial transcriptomic platforms in relation to classical histochemistry and cytochemistry. Illustrative analyses of human GBM tissue demonstrate that spatial transcriptomics robustly captures disease-relevant gene expression patterns and enables comprehensive mapping of key pathological features, including pseudopalisading necrosis, aberrant tumor vasculature, and therapy-resistant tumor niches. When integrated with histopathological observations, spatially resolved transcriptomic data can generate biologically meaningful hypotheses, offering insight into immune suppression, and proliferative signaling networks. These examples underscore the potential of spatial transcriptomics to bridge morphology and molecular biology, thereby expanding the conceptual framework of histopathological research. At the same time, spatial transcriptomic data should not be regarded as a replacement for direct microscopic evaluation. Limitations in morphological fidelity, lack of subcellular resolution, indirect inference of functional states, and reliance on computational interpretation necessitate careful integration with established histochemical and immunohistochemical methods. Without a solid foundation in tissue and cellular morphology, spatial transcriptomic findings may be misinterpreted or overstated. Collectively, this review emphasizes that spatial transcriptomics and histochemistry are complementary approaches, whose effective integration depends critically on rigorous histochemical knowledge to ensure accurate pathological interpretation and translational relevance.

Key words: spatial transcriptomics, glioblastoma, transcription, review

I. Introduction

Spatial transcriptomics has emerged as a transformative approach for bridging molecular information with tissue morphology, enabling comprehensive gene expression profiling while preserving the architectural context that has

Correspondence to: Sohei Kitazawa, MD PhD, Department of Molecular Pathology, Ehime University Graduate School of Medicine, Shitsukawa, Toon City, Ehime 562–0295, Japan. E-mail: kitazawa@m.ehime-u.ac.jp

long been central to histochemistry [1–3]. Among these technologies, the recently introduced high-resolution spatial transcriptomics platforms such as Visium HD allow genome-wide transcriptional mapping directly on histological sections, thereby providing a unique opportunity to examine cellular heterogeneity, microenvironmental organization, and pathological architecture *in situ* [1, 3–5]. This integration of molecular readouts with preserved tissue structure is particularly appealing for neuropathological specimens, in which cytoarchitecture and regional microenvironments profoundly shape disease behavior [6, 7].

From the standpoint of histochemistry, high-resolution spatial transcriptomics platforms offer several clear advantages. They provide unbiased transcriptome-wide data, overcoming the inherently targeted nature of classical *in situ* hybridization (ISH) or immunohistochemistry [8, 9]. The spatial barcoding strategy captures transcriptional patterns across broad tissue regions, enabling the reconstruction of delicate tumor-stroma-vascular interactions in ways not easily achievable by conventional serial or multiplex staining [10, 11]. In highly heterogeneous lesions such as glioblastoma multiforme (GBM), where proliferative niches, hypoxic zones, infiltrative fronts, and tumor-immune interfaces coexist in a complex spatial mosaic, such comprehensive mapping yields insights that are not accessible through traditional morphology alone [6].

However, Visium and Visium HD also present limitations that must be recognized, particularly from a histochemical perspective. Although high-resolution spatial transcriptomics platforms substantially improve spatial resolution, neither platform currently matches the single-cell and subcellular precision of histological, immunohistochemical, or single-molecule ISH methods [12–14]. Capture-based transcript localization does not reflect the true intracellular distribution of RNA, and data quality remains sensitive to fixation conditions and RNA integrity, especially in FFPE tissues [15, 16]. These considerations highlight the importance of interpreting spatial transcriptomic data in conjunction with established morphological and cytochemical techniques, rather than viewing them as standalone replacements [17, 18].

GBM, with its pronounced intratumoral diversity and microenvironmental complexity, represents an ideal tissue context in which to evaluate both the strengths and the constraints of high-resolution spatial transcriptomics platforms [6]. By integrating spatial transcriptomic findings with classical histochemical observations, it becomes possible to refine existing pathological concepts and uncover new layers of biological organization within the tumor [19].

In this review, we draw on our high-resolution spatial transcriptomics platforms of human GBM tissue to critically examine the practical advantages and limitations of high-resolution spatial transcriptomics, and to outline how these technologies can be integrated with traditional histochemistry to establish a coherent and synergistic framework for future neuro-oncologic investigation.

II. Illustrative Analysis of GBM by Visium HD Spatial Transcriptomics

Tissue selection

As an illustrative example in this review, a representative case of GBM (A female patient in her late 60s presenting with a previously untreated primary lesion), was selected from surgically resected specimens obtained with comprehensive informed consent at Ehime University Hospital. The tissue was fixed in 10% neutral buffered formalin for 24 hr and subsequently embedded in paraffin. Histopathological examination of this case revealed the characteristic features of GBM, including pseudopalisading necrosis and prominent vascular structures composed of atypical endothelial cells with markedly enlarged and pleomorphic nuclei. Immunohistochemistry revealed negative staining for IDH1 and complete loss of p53 expression. RNA was extracted from formalin-fixed, paraffin-embedded tissue sections. The RNA sample was assessed by Distribution Value 200 (DV200), and only samples meeting the DV200 criterion (>200 nt) were used for downstream Visium HD analysis. Current RNA sample showed a DV200 value of 30–50% and an RNA integrity number (RIN) of 2.30. In Visium HD analysis, gene expression differences are quantified by the log2 fold change (L2FC), which represents the estimated logarithmic ratio of expression levels within a given cluster relative to all other spots, together with a corresponding p value assessing statistical significance. An L2FC value of 1.0 indicates a twofold increase in expression within the target cluster. Statistical significance is evaluated using a negative binomial test with multiple testing correction by the Benjamini-Hochberg method. The number of top features displayed for each cluster (N) is defined to limit the total number of table entries to 10,000 and is calculated as $N = 10{,}000/K^2$, where K denotes the total number of clusters, resulting in a range of 1–50 features per cluster. To ensure robustness, features are further filtered by a mean UMI count greater than 1.0, and those with an L2FC < 0 or an adjusted p value ≥ 0.10 are shown in gray. In our representative GBM case, Visium HD analysis detected an average of 234.5 genes per bin at 8 μm resolution and 829.7 genes per bin at 16 μm resolution, demonstrating substantial transcriptomic coverage even at higher spatial resolution. The data was visualized and interrogated using Loupe Browser v9. Based on spatial gene expression profiling, the GBM tissue and the adjacent non-tumorous brain parenchyma were classified into 13 distinct clusters (Fig. 1). When the top-ranked genes characterizing the tumor cell-dominant cluster (Cluster 1) were queried in PubMed using the key word “glioblastoma” or “glioma”, the majority were found to have been previously reported in earlier studies (Table 1). These findings indicate that Visium HD robustly captures tissue- and disease-relevant gene expression signatures, thereby supporting the reproducibility and biological validity of this spatial transcriptomic platform.

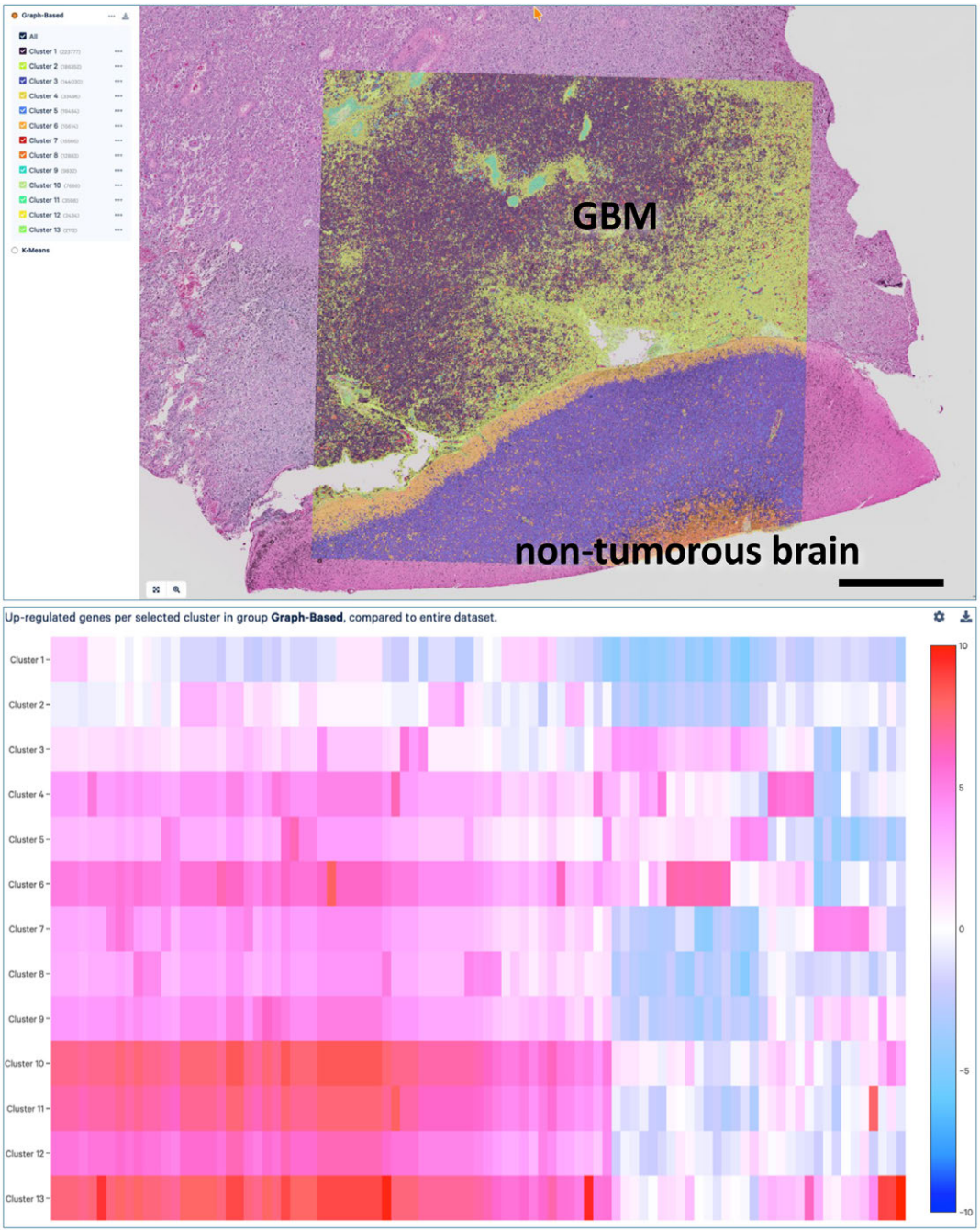

Fig. 1. Overview of the analyzed case and summary of Visium HD-based spatial transcriptomic analysis. The upper panel shows representative histopathological findings of glioblastoma multiforme (GBM). A 5-mm square region of interest encompassing the boundary between non-tumorous and tumorous areas was selected for Visium HD spatial transcriptomic analysis. Using Loupe Browser v9, the dataset was classified into 13 distinct clusters. The lower panel presents heat maps of gene expression patterns for each cluster. Bar = 1 mm.

Although the present Visium analysis was performed on a single representative GBM case, and any direct inductive generalization to GBM as a whole must therefore be approached with caution, extending such comprehensive spatial analyses into a morphological framework offers several important advantages. These merits are discussed in Section III, while the current limitations of this approach are addressed in Section IV.

III. Exploratory Power of Spatially Comprehensive Transcriptomics in Histochemical Contexts

Beyond reproducibility, high-resolution spatial transcriptomics offer a comprehensive and unbiased exploratory framework that enables the identification of spatially restricted gene expression patterns and can yield

Table 1. *Literature frequency (as of December 2025) of the top 10 genes characterizing cluster 1*

Featured Gene	Glioblastoma	Glioma
DHH	7	16
POMC	23	89
COL20A1	0	2
BMP5	1	2
BMP8B	0	0
MIA	48	43
ITGB3	13	17
RNF128	0	0
TNFRSF19	8	11
GLP1R	2	4

For each gene, the number of publications retrieved by PubMed searches using the terms “glioblastoma” or “glioma” is shown, indicating the extent to which these genes have been previously associated with glioma-related studies.

unexpected conceptual seeds suggestive of biologically meaningful interactions. In this regard, such insights may serve as a source of inspiration and motivation for the generation of new research hypotheses. In the present analysis, we aimed to dissect the cellular composition and biological significance of the pseudopalisading pattern in GBM pathology, to delineate the properties of tumor vasculature composed of enlarged and atypical endothelial cells, and to identify potential factors that may contribute to therapeutic resistance in GBM. Through this approach, we identified several lines of inquiry that may serve as novel research seeds, as outlined below.

Visium HD-based analysis of pseudopalisading necrosis (Fig. 2)

The pseudopalisading necrotic architecture (Fig. 2A) was primarily characterized by Cluster 11 (Fig. 2B), corresponding to the necrotic core, and Cluster 2, representing tumor cells arranged in a palisading pattern surrounding the necrosis (Fig. 2B). Cluster 11 was enriched for genes typically expressed in macrophage-lineage cells, including CXCL12, S100A4, S100A9, and SPP1, consistent with the cellular composition of necrotic foci. In contrast, as shown in the heat map in lower panel of Figure 2, tumor cells adjacent to the necrotic areas (Cluster 2) exhibited distinct molecular properties compared with tumor cells located elsewhere (Cluster 1). Genes significantly upregulated in Cluster 2 relative to Cluster 1 included MYF5, DDX3Y, C13orf46, TMCO3, HOXA13, and FOXN1, whereas KRTAP10-1, IRX4, KRTAP21-1, PMB2, UBE2U, and SMR3A were significantly downregulated. Notably, several of the genes upregulated in Cluster 2 have been reported to be epigenetically regulated under physiological conditions [20–26]. These findings suggest that epigenetic alterations induced by the perinecrotic microenvironment may promote a deviation from the canonical neural differentiation identity of tumor cells, potentially reflecting lineage infidelity or a shift toward a stem-like or progenitor-like cellular state.

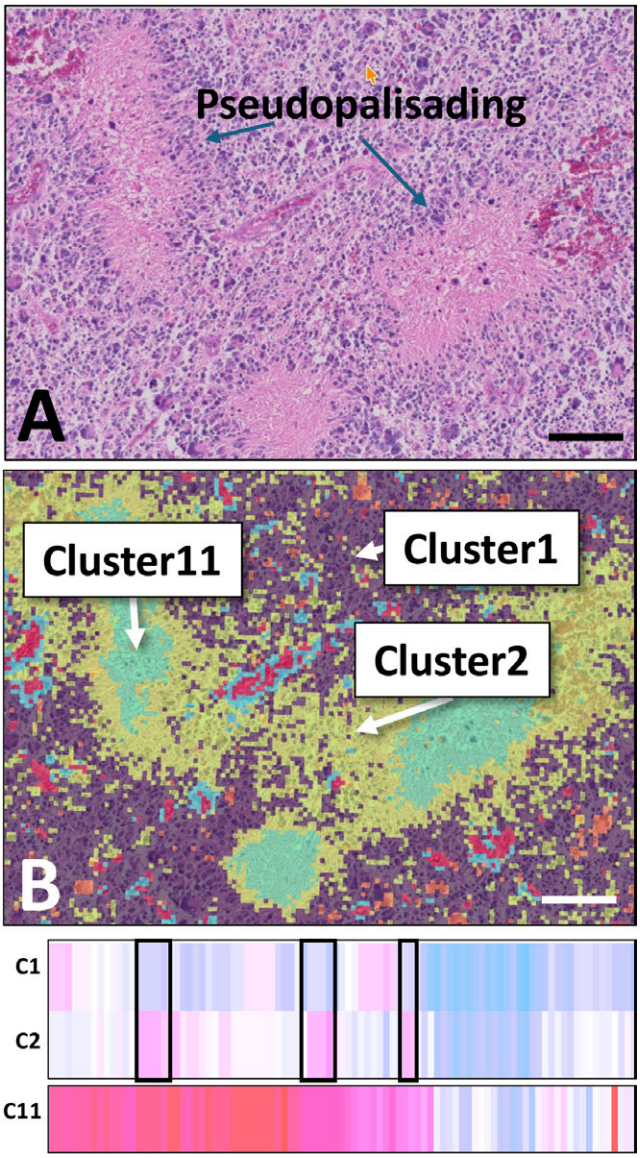

Fig. 2. Spatial transcriptomic analysis of pseudopalisading necrosis. (**A**) The hematoxylin and eosin–stained image shows an eosinophilic necrotic area with a paucity of cellular components within the tumor tissue. Surrounding this necrotic core, tumor cells are arranged in a cord-like pattern, forming the characteristic pseudopalisading architecture. (**B**) Spatial transcriptomic analysis revealed that the necrotic area was classified as cluster 11, whereas pseudopalisading tumor cells were assigned to cluster 2, and the background tumor tissue to cluster 1. In the heat map analysis shown below, comparison between cluster 1 (C1) and cluster 2 (C2) demonstrates that a subset of genes, highlighted by black boxes, shifts from low expression (blue) to higher expression (red), suggesting activation of specific gene programs in C2. Genes predominantly expressed in cluster 11 (C11) are inferred to originate largely from macrophages within the necrotic area. Although cluster 2 is spatially adjacent to cluster 11 and some gene expression in C2 may reflect macrophage-derived signals, the altered gene set is limited to specific genes, indicating that the majority of the expression changes observed in C2 are likely derived from tumor cells. Bars = 150 μm.

Comparison of aberrant intratumoral vasculature and non-neoplastic vessels by high-resolution spatial transcriptomics

One of the hallmark histopathological features of glioblastoma is the presence of aberrantly proliferated and highly disorganized vascular structures, often forming complex, multilayered tufts that resemble renal glomeruli and are therefore referred to as glomeruloid vessels [27]. In this context, two landmark studies published simultaneously in Nature in December 2010 fundamentally reshaped the prevailing concept of tumor vascularization by demonstrating that glioblastoma stem-like cells can differentiate into endothelial cells and directly contribute to the formation of tumor vasculature [28, 29]. Prior to these reports, intratumoral blood vessels were generally believed to arise predominantly through angiogenic sprouting from pre-existing normal vasculature. They provided compelling genetic and functional evidence that a substantial fraction of endothelial cells within glioblastoma–ranging from approximately 20% to as high as 90% in certain cases–harbor the same oncogenic alterations as the tumor cells themselves [28]. Moreover, CD133-positive glioma stem-like cells were shown to possess the capacity to transdifferentiate not only into neural lineages but also into vascular endothelial cells [29]. This paradigm-shifting concept offered a mechanistic explanation for the limited and often transient efficacy of conventional anti-angiogenic therapies, such as bevacizumab, by implicating tumor cell-derived vasculature as a source of intrinsic or acquired therapeutic resistance [30]. Collectively, these findings underscored the need for therapeutic strategies that directly target cancer stem-like cells or disrupt their endothelial differentiation program as a potentially more durable approach to glioblastoma treatment. In the present Visium HD analysis, vascular structures in non-neoplastic regions were classified into cluster 13 (Fig. 3A), whereas intratumoral glomeruloid vessels were segregated into clusters 7 and 9 (Fig. 3B). Heat map analysis (Fig. 3C) revealed that these vascular clusters exhibited an intermediate transcriptional profile between the representative tumor cell clusters (clusters 1 and 2) and the background non-neoplastic vascular cluster (cluster 13). This intermediate pattern supports the notion that a substantial proportion of intratumoral vessels are formed through phenotypic conversion of tumor cells themselves, rather than arising solely from pre-existing normal vasculature.

Dissecting therapeutic resistance in glioblastoma by high-resolution spatial transcriptomics: targeted gene analysis and unbiased spatial region discovery

TOP2A-LGALS1-immune microenvironment axis

DNA topoisomerase IIα (TOP2A) is used as a representative example of targeted gene analysis. Building on evidence that TOP2A is highly expressed in glioblastoma and associated with aggressive behavior, poor prognosis, and therapeutic resistance [31, 32], we investigated GBM treatment resistance from a tumor-immune interaction perspective. Because TOP2A overexpression reflects proliferative stress and genomic instability, features increasingly linked to immune evasion [33], spatial analysis enables localization of TOP2A-high tumor compartments in relation to immune cell distribution and microenvironmental states. Integration of high-resolution spatial transcriptomics platforms data with histopathological context allows dissection of how treatment-refractory, highly proliferative tumor niches overlap with immunosuppressive or immune-excluded regions, providing insight into the spatial coupling of cell-cycle dysregulation, immune escape, and therapeutic failure in GBM.

Spatial transcriptomic analysis revealed that TOP2A and lectin, galactoside-binding, soluble, 1; galectin-1 (LGALS1) were broadly upregulated throughout the tumor tissue (Fig. 4A). Importantly, subsequent immunohistochemical analysis by use of (rabbit polyclonal antibody to TOP2A (Proteintech, 20233-1-AP, at 1:400 dilution) and to Galectin-1 (Proteintech, 11858-1-AP, at 1:1000 dilution) provided additional spatial resolution at the protein level, demonstrating that both TOP2A and LGALS1 showed particularly enhanced expression in tumor cells located in close proximity to microvessels (Fig. 4B). These immunohistochemical findings refine the transcriptomic observations by highlighting the perivascular enrichment of these proteins within the tumor microenvironment. Further combined analyses focusing on LGALS1, CD69, and immune cell markers revealed that CD69 and CD4 were expressed at lower levels in tumor tissue compared with adjacent non-tumorous regions (Fig. 4A). Importantly, this reduction in expression was independently confirmed by immunohistochemical analysis, which demonstrated decreased immunoreactivity for CD69 and CD4 within the tumor tissue (Fig. 4B). Previous studies have shown that LGALS1 can suppress the differentiation of Th17 cells through its interaction with CD69 [34, 35]. Taken together, our findings support a model in which increased LGALS1 expression in the GBM microenvironment dampens $CD4^+$ T-cell-related immune signaling [36]. Overall, the data suggests that infiltration of peripheral myeloid cells and the development of an immune-tolerant environment promote LGALS1 upregulation, thereby contributing to immune suppression and tumor progression in glioblastoma. Although the precise mechanism by which TOP2A influences LGALS1 remains unclear, our findings raise the possibility that the characteristic upregulation of LGALS1 in TOP2A-high tumor cells contributes, at least in part, to resistance against immunotherapy in GBM.

Identification of genes downregulated in tumor tissue compared with non-neoplastic tissue

As an example of unbiased spatial region discovery, a heat map analysis was performed comparing cluster 1, corresponding to tumor tissue, with cluster 3, which predominantly comprised glial cells in the non-tumorous region (Fig. 5A). Differential expression analysis between these two clusters is shown in Figure 5B. Among genes exhibit-

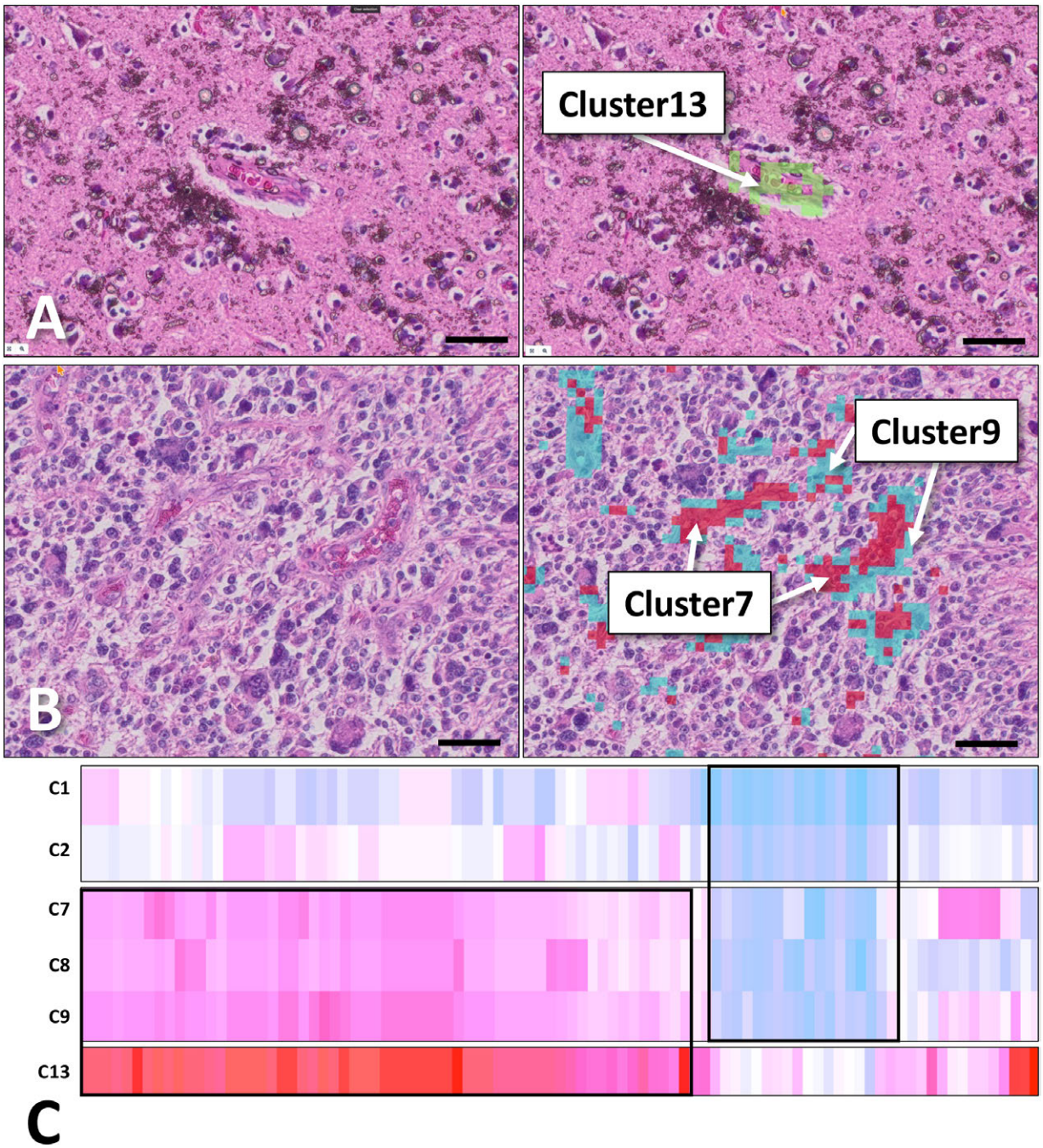

Fig. 3. Spatial transcriptomic analysis of vascular characteristics in non-tumorous and tumorous regions. (**A**) The left panel shows vascular structures within non-tumorous brain tissue. As indicated in the right panel, these vascular structures were classified as cluster 13. (**B**) The left panel shows vascular structures observed within the tumor, in which marked nuclear enlargement of endothelial cells is evident. Although not shown in this panel, these vessels often exhibit the glomeruloid architecture characteristic of glioblastoma multiforme (GBM). Tumor-associated vascular structures were classified into clusters 7 and 9. (**C**) The heat map analyses among clusters predominantly represent tumor tissue (clusters 1 and 2; C1 and C2), tumor-associated vascular structures (clusters 7 and 9; C7 and C9), and non-tumorous vascular structures (cluster 13; C13). Clusters C7 and C9 shared a largely overlapping set of low-expression genes (shown in blue; upper right boxed area) with clusters C1 and C2. In contrast, many high-expression genes (shown in red; lower left boxed area) exhibited expression patterns similar to those observed in non-tumorous vascular structures (C13). Although this analysis does not rely on mutation-based markers, the vascular structures formed within the tumor display features characteristic of both tumor tissue and non-neoplastic vasculature. These findings support previous reports suggesting that a substantial proportion of tumor-associated vessels arise through phenotypic alteration of tumor cells. Bars = 75 μm.

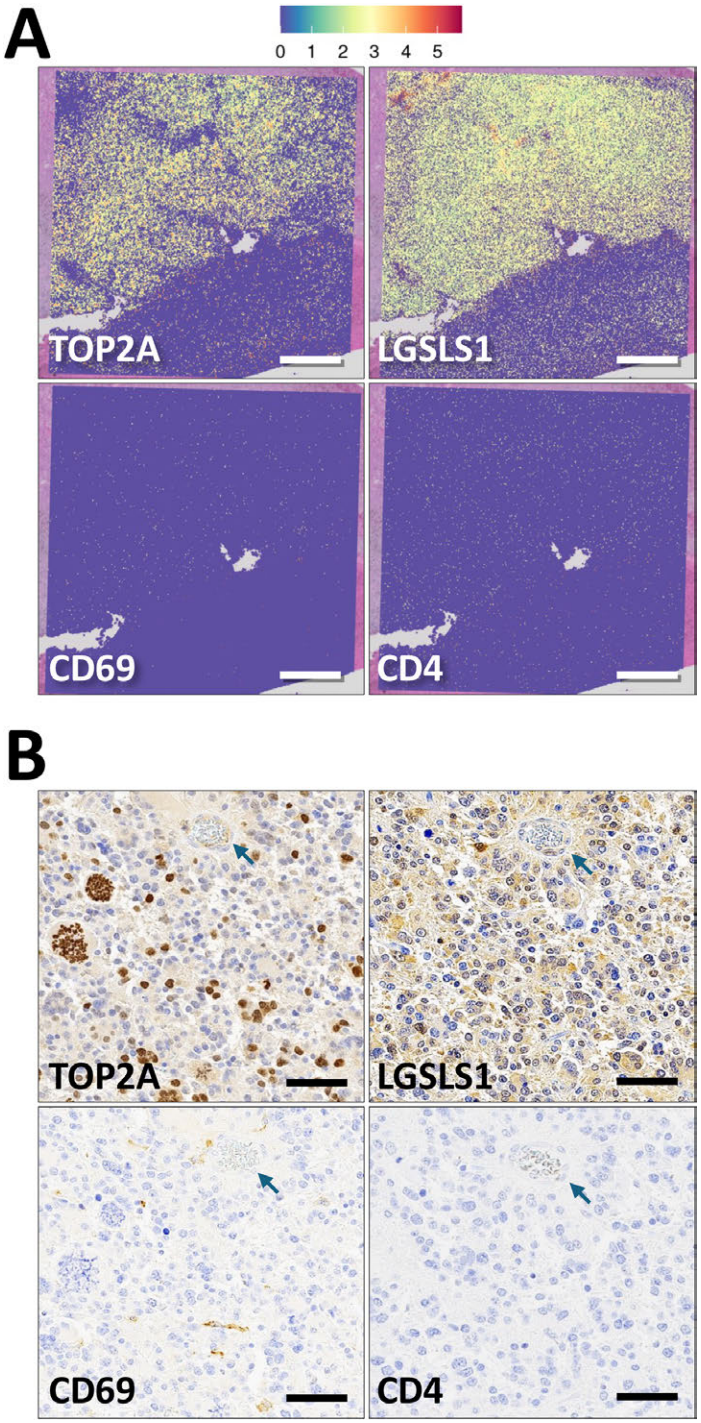

Fig. 4. Spatial transcriptomics-based *in situ* hybridization–like expression mapping of the TOP2A-LGALS1-immune microenvironments axis and validation by immunohistochemistry. (**A**) To simulate an *in situ* hybridization–like pattern, spatial transcriptomic data for TOP2A, LGALS1, CD69, and CD4 were mapped onto the tissue section. TOP2A and LGALS1 expression was markedly upregulated in the tumor region compared with the non-tumorous area located in the lower right of the section. In contrast, no corresponding increase in the expression of CD69 or CD4, which are presumed to be negatively regulated by LGALS1, was observed. Bars = 1 mm. (**B**) Immunohistochemical staining using specific antibodies against TOP2A, LGALS1, CD69, and CD4 demonstrated expression patterns parallel to those observed in panel (**A**), confirming that the mRNA expression profiles identified by spatial transcriptomics are similarly reflected at the protein level. Microvessels are indicated by arrows. Bars = 75 µm.

ing marked differences in expression, the region highlighted in red indicates genes upregulated in tumor tissue, whereas the region highlighted in blue represents genes downregulated in tumor tissue. Within the downregulated gene set highlighted in blue, Wnt inhibitory factor 1 (WIF1) was ranked at the top of the list. Spatial mapping of

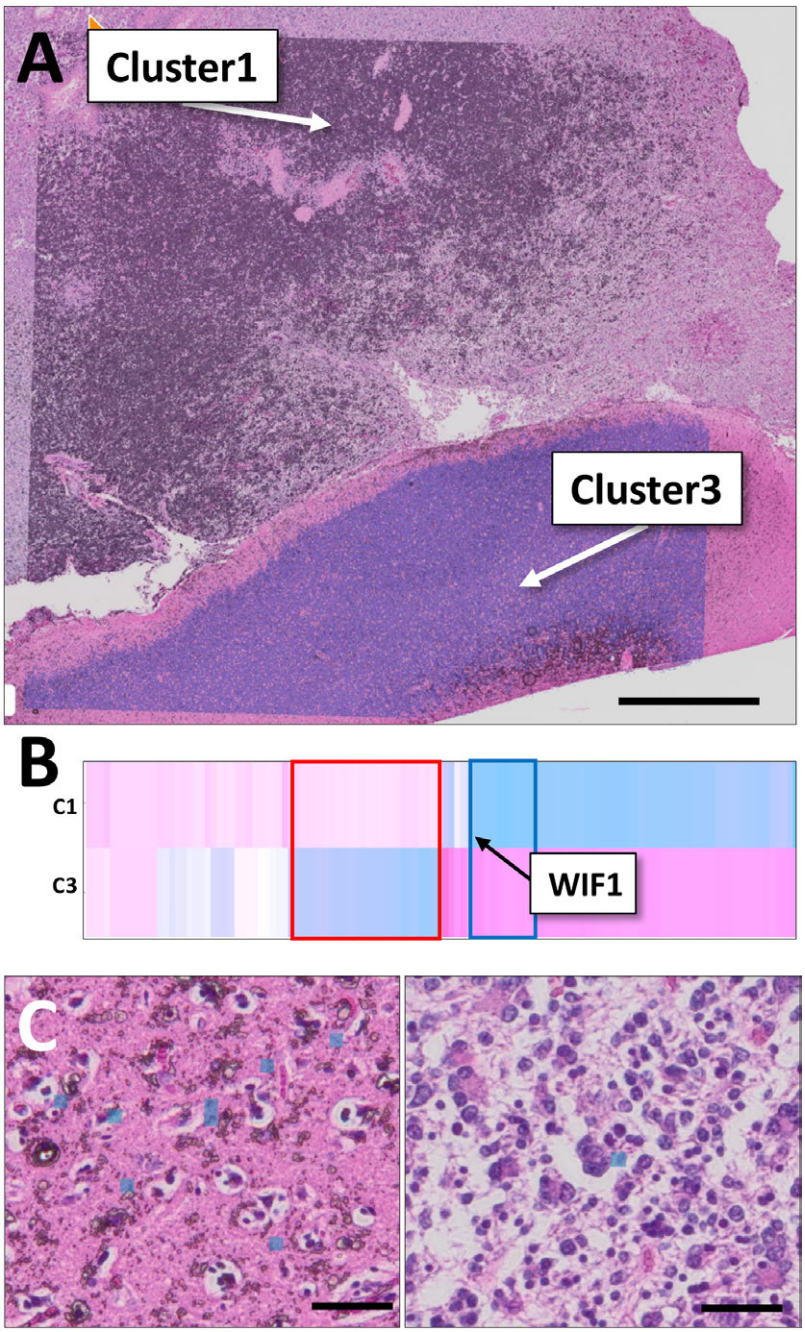

Fig. 5. Unbiased spatial region–based identification of genes downregulated in tumor tissue. (**A**) Spatial clustering analysis identifying cluster 1 corresponding to tumor tissue and cluster 3 predominantly composed of glial cells in the non-tumorous region. (**B**) Heat map showing differential gene expression between cluster 1 and cluster 3. Genes upregulated in tumor tissue are highlighted in red, whereas genes downregulated in tumor tissue are highlighted in blue. Bar = 1 mm. (**C**) Spatial expression mapping of Wnt inhibitory factor 1 (WIF1). Numerous cyan-colored expression spots are observed in the non-tumorous region (left), whereas WIF1 expression is markedly reduced in the tumor region (right). Bars = 75 µm.

WIF1 expression demonstrated numerous cyan-colored expression spots in the non-tumorous region (Fig. 5C, left), whereas its expression was markedly reduced in the tumor region (Fig. 5C, right). Consistent with this observation, previous studies have identified WIF1 as a candidate tumor suppressor gene in GBM, located within the chromosomal region 12q13–12q15 flanked by MDM2 and CDK4. Notably, the blue-highlighted region in Figure 5B is likely to contain multiple genes that have not yet been extensively characterized in GBM. These genes may therefore represent potential sources of novel therapeutic targets identified through unbiased spatial transcriptomic analysis.

Thus, high-resolution spatial transcriptomics platforms enable gene expression profiling that can be guided by the

morphological characteristics of tissues and cells, allowing investigators to link histological features with their underlying molecular signatures. Conversely, it also permits a gene-centered approach, in which attention to the expression of specific genes can be expanded to explore the corresponding cellular and tissue-level features. In this way, high-resolution spatial transcriptomics platforms serve as a powerful bridge between classical morphology and molecular biology, facilitating integrated interpretation in histopathological research.

IV. Limitations of Spatially Comprehensive Approaches from a Histochemical View

High cost of spatial transcriptomics

Although recent advances have enabled near-cellular resolution and multi-omics integration in spatial transcriptomics, these approaches require substantial financial investment, specialized instrumentation, and extensive computational resources, which remain major barriers to widespread adoption. For laboratories operating under limited research budgets, investing in spatial transcriptomics inevitably represents a form of risk. To minimize the possibility of failure–such as generating data that do not address the intended biological question–researchers are compelled to exercise extreme caution in specimen selection, determination of regions of interest, and decisions regarding tissue trimming and inclusion within the limited analytical area. This constraint is especially restrictive for early-career investigators at the start-up stage, who may have innovative research ideas but are understandably hesitant to allocate a large proportion of their funding to a single, costly spatial transcriptomics experiment. To foster broader and more equitable adoption of these technologies, enhanced research funding schemes, along with the development of shared platforms such as open-access data repositories and community-wide data-sharing infrastructures, are critically needed.

Limited preservation of diagnostic morphological fidelity

Although spatial transcriptomic technologies such as Visium HD have achieved higher spatial resolution in recent years, they still have inherent limitations in capturing the fine structural details that are critical for histopathological interpretation [37, 38]. Traditional histochemical and immunohistochemical methods remain superior for clearly visualizing nuclear shape, chromatin organization, cell boundaries, stromal structure, and subtle changes such as necrosis or fibrosis. By contrast, spatial omics data reflect molecular information averaged within defined spatial units and therefore cannot replace direct microscopic examination of tissue architecture, which remains the foundation of diagnostic and interpretive pathology.

Inability to resolve subcellular localization

Conventional immunohistochemistry and *in situ* hybridization enable direct visualization of molecular localization at the subcellular level, distinguishing nuclear, cytoplasmic, membranous, or polarized distributions within individual cells [39]. Such spatial precision is critical for interpreting signaling pathways, transcriptional regulation, and cellular polarity. Spatial transcriptomics approaches near-single-cell resolution but does not retain information on intracellular compartmentalization, representing an intrinsic limitation when compared with classical histochemical methodologies.

Reduced molecular specificity at the single-target level

Spatially comprehensive approaches prioritize breadth and throughput, often at the expense of target-specific interpretability. In contrast, immunohistochemistry and sequence-specific *in situ* methods rely on rigorously validated antibodies or probes, allowing direct detection of defined proteins, nucleic acid sequences, or epigenetic modifications within preserved tissue context [40]. This distinction is particularly relevant for post-translational modifications and chemical alterations, such as DNA methylation, which cannot be inferred reliably from transcript abundance alone [41].

Indirect representation of functional states

Histochemical techniques can directly visualize functional cellular states, including enzyme activity, cell cycle progression, apoptosis, extracellular matrix composition, and tissue remodeling [16]. These features often represent downstream phenotypic consequences rather than transcriptional events. Spatial transcriptomics requires such functional states to be inferred computationally from gene expression signatures, introducing an additional interpretive layer and potential ambiguity that is absent in direct histochemical observation [37].

Limited long-term reproducibility and routine applicability

Traditional histochemical and immunohistochemical methods are well standardized, broadly reproducible across institutions, and compatible with long-term archival tissue analysis [16]. Their robustness has enabled consistent diagnostic application and retrospective studies over decades. In contrast, spatial omics platforms depend heavily on evolving analytical pipelines, reference datasets, and software ecosystems, which may limit long-term reproducibility, cross-study comparability, and immediate integration into routine histopathological practice.

Restricted capacity for hypothesis-driven validation

Spatial transcriptomics excels as a hypothesis-generating tool by providing unbiased, global molecular landscapes. However, definitive hypothesis testing–addressing whether a specific molecule operates within a defined cell type, structure, or microenvironment–still relies on conventional histochemical validation [16]. Immunohistochemistry and related techniques remain

indispensable for confirming causative associations suggested by spatial omics, underscoring their continued central role in mechanistic and translational pathology research [19].

Histochemical validation at the protein level or the need for multi-omics integration

As is well recognized, analysis of mRNA expression alone cannot capture functionally critical information, such as the enzymatic activity of proteins or dynamic changes in the subcellular localization of membrane receptors within the plasma membrane, cytoplasm, or nucleus [16]. For this reason, complementary histochemical approaches–most notably immunohistochemistry–are required to achieve analyses that are more directly linked to biological function [16]. While spatial transcriptomics provide an extraordinarily rich source of information and generates numerous promising research leads, their validation inevitably depends on careful, stepwise histochemical work, beginning with the acquisition and validation of specific antibodies. Such meticulous histochemical efforts remain indispensable for translating transcriptomic insights into functionally meaningful biological understanding.

V. Perspective

Our present data on GBM illustrate that high-resolution spatial transcriptomics platforms provide reproducible and biologically meaningful spatial transcriptomic information and excels in uncovering spatial gene expression patterns that generate testable mechanistic hypotheses. However, to fully exploit this technology, it is essential that fundamental histological knowledge be integrated with an understanding of biological processes and the spatial localization of molecular components, thereby enabling coherent interpretation of spatial transcriptomic data within a rigorous morphological framework.

VI. Conflicts of Interest

The authors have no conflicts of interest.

VII. Author Contributions

S. Tomioka, R. Haraguchi, and Y. Takaoka performed the molecular experiments and analyzed the data. R. Kitazawa conducted the pathological diagnosis. A. Inoue carried out the clinical evaluation. S. Kitazawa designed and coordinated the research and wrote the manuscript.

VIII. Acknowledgments

Supported by a Grant-in-Aid for Scientific Research from the Ministry of Education, Culture, Sports, Science and Technology, Japan (22K06981, 23K20314, 24K02251)

IX. References

1. Stahl PL, Salmen F, Vickovic S, Lundmark A, Navarro JF, Magnusson J, et al. Visualization and analysis of gene expression in tissue sections by spatial transcriptomics. Science. 2016;353(6294):78–82.
2. Tian L, Chen F, Macosko EZ. The expanding vistas of spatial transcriptomics. Nat Biotechnol. 2023;41(6):773–782.
3. Rodriques SG, Stickels RR, Goeva A, Martin CA, Murray E, Vanderburg CR, et al. Slide-seq: A scalable technology for measuring genome-wide expression at high spatial resolution. Science. 2019;363(6434):1463–1467.
4. Oliveira MF, Romero JP, Chung M, Williams SR, Gottscho AD, Gupta A, et al. High-definition spatial transcriptomic profiling of immune cell populations in colorectal cancer. Nat Genet. 2025;57(6):1512–1523.
5. Vickovic S, Eraslan G, Salmen F, Klughammer J, Stenbeck L, Schapiro D, et al. High-definition spatial transcriptomics for in situ tissue profiling. Nat Methods. 2019;16(10):987–990.
6. Ma S, Sun Y, Zheng S, Fu Y, Wang L, Liu D, et al. Single-cell and spatial atlas of glioblastoma heterogeneity: characterizing the PCLAF+ subtype and YEATS4's oncogenic role. Front Immunol. 2025;16:1614549.
7. Maynard KR, Collado-Torres L, Weber LM, Uytingco C, Barry BK, Williams SR, et al. Transcriptome-scale spatial gene expression in the human dorsolateral prefrontal cortex. Nat Neurosci. 2021;24(3):425–436.
8. Chen TY, You L, Hardillo JAU, Chien MP. Spatial Transcriptomic Technologies. Cells. 2023;12(16):2042.
9. Lein E, Borm LE, Linnarsson S. The promise of spatial transcriptomics for neuroscience in the era of molecular cell typing. Science. 2017;358(6359):64–69.
10. Wu SZ, Al-Eryani G, Roden DL, Junankar S, Harvey K, Andersson A, et al. A single-cell and spatially resolved atlas of human breast cancers. Nat Genet. 2021;53(9):1334–1347.
11. Qi J, Sun H, Zhang Y, Wang Z, Xun Z, Li Z, et al. Single-cell and spatial analysis reveal interaction of FAP(+) fibroblasts and SPP1(+) macrophages in colorectal cancer. Nat Commun. 2022;13(1):1742.
12. Lee J, Yoo M, Choi J. Recent advances in spatially resolved transcriptomics: challenges and opportunities. BMB Rep. 2022;55(3):113–124.
13. Marx V. Method of the Year: spatially resolved transcriptomics. Nat Methods. 2021;18(1):9–14.
14. Chen KH, Boettiger AN, Moffitt JR, Wang S, Zhuang X. RNA imaging. Spatially resolved, highly multiplexed RNA profiling in single cells. Science. 2015;348(6233):aaa6090.
15. Li H, Zhou J, Li Z, Chen S, Liao X, Zhang B, et al. A comprehensive benchmarking with practical guidelines for cellular deconvolution of spatial transcriptomics. Nat Commun. 2023;14(1):1548.
16. Koji T. Reflections on the Principles of Fixation in Histochemistry and Cytochemistry: With a Special Focus on Immunohistochemistry and In Situ Hybridization. Acta Histochem Cytochem. 2025;58(2):31–43.
17. Chelebian E, Avenel C, Wahlby C. Combining spatial transcriptomics with tissue morphology. Nat Commun. 2025;16(1):4452.
18. Isnard P, Humphreys BD. Spatial Transcriptomics: Integrating Morphology and Molecular Mechanisms of Kidney Diseases. Am J Pathol. 2025;195(1):23–39.
19. Kitazawa S, Takeshita E, Tomida H, Miyake T, Ikeda Y, Bekku S, et al. Spatial transcriptomic analysis of foveolar-type gastric adenoma with raspberry-like appearance. Virchows Arch. 2025, doi: 10.1007/s00428-025-04302-3.

20. Innocenzi A, Latella L, Messina G, Simonatto M, Marullo F, Berghella L, et al. An evolutionarily acquired genotoxic response discriminates MyoD from Myf5, and differentially regulates hypaxial and epaxial myogenesis. EMBO Rep. 2011;12(2):164–171.
21. Li G, Zeng H, Ru G, Yin F, Liu S, He J. WTAP regulates DDX3Y mRNA via m6A modification to promote high glucose-induced podocytes injury and diabetic nephropathy progression. Gen Physiol Biophys. 2025;44(5):405–417.
22. Li X, Han M, Zhu H, Pan Y, Su C, Liu Y, et al. m(6)A-Mediated TMCO3 Promotes Hepatocellular Carcinoma Progression by Facilitating the Membrane Translocation and Activation of AKT. Adv Sci (Weinh). 2025;12(27):e2504187.
23. Feng W, Chen T. Epigenetic modification mediated by PHF20/METTL14/HOXA13 signaling axis modulates osteogenic differentiation of mesenchymal stem cells. Funct Integr Genomics. 2025;25(1):7.
24. Kadouri N, Givony T, Nevo S, Hey J, Ben Dor S, Damari G, et al. Transcriptional regulation of the thymus master regulator Foxn1. Sci Immunol. 2022;7(74):eabn8144.
25. Chakma K, Gu Z, Abudurexiti Y, Hata T, Motoi F, Unno M, et al. Epigenetic inactivation of IRX4 is responsible for acceleration of cell growth in human pancreatic cancer. Cancer Sci. 2020; 111(12):4594–4604.
26. Alghanim H, Balamurugan K, McCord B. Development of DNA methylation markers for sperm, saliva and blood identification using pyrosequencing and qPCR/HRM. Anal Biochem. 2020; 611:113933.
27. Haddad SF, Moore SA, Schelper RL, Goeken JA. Vascular smooth muscle hyperplasia underlies the formation of glomeruloid vascular structures of glioblastoma multiforme. J Neuropathol Exp Neurol. 1992;51(5):488–492.
28. Ricci-Vitiani L, Pallini R, Biffoni M, Todaro M, Invernici G, Cenci T, et al. Tumour vascularization via endothelial differentiation of glioblastoma stem-like cells. Nature. 2010; 468(7325):824–828.
29. Wang R, Chadalavada K, Wilshire J, Kowalik U, Hovinga KE, Geber A, et al. Glioblastoma stem-like cells give rise to tumour endothelium. Nature. 2010;468(7325):829–833.
30. Brandes AA, Gil-Gil M, Saran F, Carpentier AF, Nowak AK, Mason W, et al. A Randomized Phase II Trial (TAMIGA) Evaluating the Efficacy and Safety of Continuous Bevacizumab Through Multiple Lines of Treatment for Recurrent Glioblastoma. Oncologist. 2019;24(4):521–528.
31. Arivazhagan A, Kumar DM, Sagar V, Patric IR, Sridevi S, Thota B, et al. Higher topoisomerase 2 alpha gene transcript levels predict better prognosis in GBM patients receiving temozolomide chemotherapy: identification of temozolomide as a TOP2A inhibitor. J Neurooncol. 2012;107(2):289–297.
32. Zhou T, Wang Y, Qian D, Liang Q, Wang B. Over-expression of TOP2A as a prognostic biomarker in patients with glioma. Int J Clin Exp Pathol. 2018;11(3):1228–1237.
33. Davoli T, Uno H, Wooten EC, Elledge SJ. Tumor aneuploidy correlates with markers of immune evasion and with reduced response to immunotherapy. Science. 2017;355(6322):eaaf8399.
34. Cibrian D, Saiz ML, de la Fuente H, Sanchez-Diaz R, Moreno-Gonzalo O, Jorge I, et al. CD69 controls the uptake of L-tryptophan through LAT1-CD98 and AhR-dependent secretion of IL-22 in psoriasis. Nat Immunol. 2016;17(8):985–996.
35. de la Fuente H, Cruz-Adalia A, Martinez Del Hoyo G, Cibrian-Vera D, Bonay P, Perez-Hernandez D, et al. The leukocyte activation receptor CD69 controls T cell differentiation through its interaction with galectin-1. Mol Cell Biol. 2014;34(13):2479–2487.
36. Verschuere T, Toelen J, Maes W, Poirier F, Boon L, Tousseyn T, et al. Glioma-derived galectin-1 regulates innate and adaptive antitumor immunity. Int J Cancer. 2014;134(4):873–884.
37. Larsson L, Frisen J, Lundeberg J. Spatially resolved transcriptomics adds a new dimension to genomics. Nat Methods. 2021;18(1):15–18.
38. Rao A, Barkley D, Franca GS, Yanai I. Exploring tissue architecture using spatial transcriptomics. Nature. 2021; 596(7871):211–220.
39. Choijookhuu N, Shibata Y, Ishizuka T, Xu Y, Koji T, Hishikawa Y. An Advanced Detection System for In Situ Hybridization Using a Fluorescence Resonance Energy Transfer-based Molecular Beacon Probe. Acta Histochem Cytochem. 2022; 55(5):119–128.
40. Kitazawa R, Haraguchi R, Murata Y, Takaoka Y, Kitazawa S. CpG Methylation of Receptor Activator NF-kappaB (RANK) Gene Promoter Region Delineates Senescence-Related Decrease of RANK Gene Expression. Acta Histochem Cytochem. 2024;57(4):137–147.
41. Esteller M. Cancer epigenomics: DNA methylomes and histone-modification maps. Nat Rev Genet. 2007;8(4):286–298.